Prepared for Inst. Phys. and
The Physical Soc., Univ.
of Oxford, London, Eng.

HIGH-FIELD MAGNETS AND MAGNETIC RESEARCH AT NASA LEWIS RESEARCH CENTER

By James C. Laurence

Lewis Research Center
National Aeronautics and Space Administration
Cleveland, Ohio

INTRODUCTION

The Lewis Research Center is involved in research on methods for propulsion and power generation to be used in space exploration. This research is of an advanced nature and involves chemical, electric, nuclear, and other types of rockets. In addition to the actual propulsion research, much support research is necessary to develop these advanced concepts. In many of these concepts, strong magnetic fields are necessary to focus or contain high-temperature plasmas or to induce voltages in them for power generation. In addition to these applications of the strong magnetic field, there is a need for high-field-strength magnets for basic research on the properties of materials. Some of these are the critical fields of superconductors, the magnetoresistance of pure metals and crystals, the Hall effect, the Zeeman effect, the nuclear-magnetic resonance and other resonance effects, and many others that will be discussed at this conference.

These two needs were enough to establish at NASA Lewis Research Center a group of research scientists who have the responsibility of producing high-strength magnetic fields and of using these fields in fundamental research. The activities of this group of researchers are described in this paper.

THE PRODUCTION OF HIGH FIELDS

The concept of the low-voltage - high-current design of electromagnets led to the procurement of a homopolar generator as a power supply for these magnets. This versatile machine is described in ref. 1. It is only necessary to say, therefore, that the power available is 3 megawatts at a maximum voltage of 38 v (fig. 1).

This machine uses liquid-metal brushes to collect the charge generated by the rotation of a steel cylinder in a magnetic field produced by a conventional motor generator. Any combination of voltage and current can be drawn from the machine within the voltage and power limits. In service, the generator has proved to be exceptionally reliable with practically no interruption of operating time for maintenance.

This machine has been used to power three high-field electromagnets to the present time, two water-cooled and one cryogenically cooled.

Water-Cooled Electromagnets

The construction of the water-cooled coils is illustrated in fig. 2. A helix was formed by machining a copper ingot into a screw and collapsing it to form a series of large thick copper turns. The flow of the water is in at the center and out radially to the periphery, where it is collected and discharged into the sewer. The water is drawn directly from the mains at a pressure of 60 lb/sq in. and requires no special treatment because of the low potential drop between turns, about 1 v or less.

The dimensions and operational characteristics of these magnets are given in table I. It can be seen that the water consumption is quite modest. Other noteworthy features of the magnets are the large ratio of total conductor volume to total volume of the coils (0.94 and 0.97), the small temperature rise of the cooling water, the radial distribution of the current (most current where it does the most good), and the amounts of energy stored per unit volume (47.9 and 31.0 j/cm^3).

Of importance to the experimenter is the volume in the field. In particular, the low-temperature physicist is interested in the volume inside a liquid-helium dewar available for low-temperature - high-field research. For such research, these magnets have clear working diameters of 1.6 and 6.0 cm, and the maximum fields available are 110 and 88.5 k gauss, respectively. For high-field research at room temperature, the volume available is, of course, much larger. In this type of operation, the working diameters are 4.6 and 8.9 cm, respectively. The magnetic fields are uniform within 95 percent over the central 10 cm of the field. A picture of the 10-cm bore water-cooled magnet is shown in fig. 3.

Cryogenically Cooled Electromagnet

In ref. 2 a large liquid-neon-cooled electromagnet is described. Since that paper was written, component parts of this electromagnet have been built and tested. Figure 4 shows the construction of the coils. The backup channel to provide support for the aluminum conductor is of stainless steel, and the spacers that form the flow channels are likewise of stainless steel. The flow of the coolant is longitudinal through the magnet coils, which are kept immersed in the coolant at all times during operation. The method of cooling is boiling heat transfer to the liquid neon.

A pair of finished coils was first tested in the liquid-hydrogen dewar shown in fig. 5. The results are shown in table II and in fig. 6. The dimensions of the coils are shown, as well as the field produced and the power and current required. The field produced, 48.6 k gauss, gave 9.4 j/cm^3 of energy stored. The field is 30 cm in diameter by 12 cm long. Extrapolation of these results indicates that the goal of 200 k gauss will probably be attained when 12 coils are available for use.

Since these initial tests, the neon refrigerator has been installed, the fabrication of the first coils has been started, and the dewar to contain the electromagnet has been constructed. Some pictures of this installation are shown in figs. 7 and 8. At the present time, the complete system is being checked and prepared for operation with 12 coils in series.

RESEARCH IN HIGH-INTENSITY MAGNETIC FIELDS

The water-cooled magnets described have proved to be very useful tools in research in superconducting alloys and intermetallic compounds; i.e., the hard superconductors. These are especially interesting because of the need for superconducting magnets that will, themselves, produce high fields. The materials of most interest have thus been Nb-Zr alloys and the intermetallic compound Nb_3Sn.

Critical Current - Critical Field Relations of Hard Superconductors

The investigations into the variation of critical current with critical field of superconductors have been concerned with wires and ribbons in short samples and small coils (solenoids) wound from ribbons and wires. Intensive research has been done with Nb_3Sn and with 25 percent and 33 percent zirconium alloys with niobium. The results of some of these experiments are shown in the curves of fig. 9. In this series of tests, a short sample of ribbon coated with Nb_3Sn was soldered to copper blocks using an ultrasonic soldering technique and indium solder.[1] The sample was mounted transversely in the field and the results obtained are shown in this figure. The circles are data taken when the field was held constant, and the current was slowly and regularly increased through the sample until normal resistance appeared. The appearance of a potential drop of 10 nanovolts across a 1-cm length was the criterion used to indicate reversion to the normal state. The successive values of I_c are shown in fig. 9(a). It can be seen that in the neighborhood of 20 k gauss the data began to scatter. A different procedure gives an insight into what was happening. In this procedure, the current through the superconducting sample in a zero field was fixed and the field was slowly and uniformly increased (diamond symbols). As shown in fig. 9(a), the sample went normal at a field intensity of 2 to 3 k gauss for a current of 40 amp. Successively larger values of current were set in the sample, and the field was increased with the results shown. Not until a current of 66 amp was set, however, did the critical field occur at a value that placed a point on the I_c-H_c curve obtained by the first test procedure. Figure 9(b) shows results for another sample of Nb_3Sn ribbon. The low-field instability was likewise apparent in this sample, as shown by the data points. A similar piece of ribbon showed no such instability when the ribbon was copper plated, as shown in fig. 10. Indeed, insufficient current was available to drive the sample normal at any field less than 60 k gauss.

The low-field instability was likewise found in Nb-Zr superconducting wire. For example, fig. 11 shows the results of similar tests on short

---

[1] These ribbon samples were obtained from the Research Laboratories of Radio Corporation of America.

samples of Nb(25)Zr wire. The copper was removed from the samples before being mounted, and the same peculiar behavior was noted. Again, in certain ranges of the applied field the critical current was smaller than the values measured for much larger fields. The curves shown are not the results of a single test on one sample of material but are typical of many tests conducted on materials processed by several manufacturers. In general, the presence of copper plating or cladding on the Nb-Zr wire had the same effect as it did in the case of Nb_3Sn (fig. 12).

The data show that if the magnetic field about the sample is large enough (>10 kg) (either an externally applied or a self-generated field), the instability does not occur, and the values for I_c fall directly on the measured I_c-H_c curve.

Hall Effect in High-Intensity Fields

The investigation of the Hall effect in high magnetic fields has been conducted with commercially available semi-conductor devices that have a large Hall coefficient. The results are shown in fig. 13. Tests were made at room temperature (fig. 13(a)) and at liquid-helium temperature (fig. 13(b)) in applied fields from 0 to 75 k gauss. The response was approximately linear at room temperature, and the sensitivity of the output to changes in field strength was good. This method has now become a secondary standard of measuring the strength of the field in the laboratory.

At 4.2° K (fig. 13(b)), the Hall output is no longer a linear function of the applied field. A periodicity becomes apparent if one plots the deviation of the 4.2° K curve from the room temperature curve as a function of the reciprocal of the field. This is shown in fig. 14. The oscillations (analogous to the DeHass-Van Alphen oscillations of magnetization) are clearly shown in this figure. The most important cause of these oscillations is a periodic variation of the density of states with magnetic field.

Figure 15 shows a number of Hall-effect devices, which have been used successfully in various experiments. The response of some of these devices in liquid helium in a magnetic field is shown in fig. 16. There is a similarity in the curves, with the DeHass-Van Alphen effect more pronounced in some of them than in others.

Magnetoresistance of Pure Metals

The magnetoresistance of aluminum, bismuth, copper, and zinc has been measured at 4.2° K in fields as high as 110 k gauss. The metals used were very pure; i.e., impurities less than 10 parts per million.

In order to select a conductor for a high-field cryogenically cooled electromagnet, one of the designer's main concerns is the magnetoresistance of the conductor. Since the material is of very high purity and is

operated at very low temperatures, all the normal terms in the resistivity are exceedingly small. Hence, the part that varies with the strength of the magnetic field accompanying the current flow is of prime importance. In some metals, this magnetic component increases almost linearly with field strength. Materials such as copper and bismuth are excellent transducers for field-strength probes. In other materials, such as aluminum, sodium, etc., the magnetoresistance saturates as the field strength is increased. These are the materials that are used as conductors in cryogenically cooled electromagnets.

Extensive measurements of the magnetoresistance of 99.999+ and 99.9983 percent pure aluminum have been made at Lewis and at the National Bureau of Standards in Boulder, Colorado. The results of some of these measurements are shown in fig. 17, which includes measurements from ref. 4 and from our own laboratory. These curves show clearly the saturation of the magnetoresistance with increasing field strength. The effect of the increase in purity of 7 to 8 parts per million has a marked effect on the results at the lower temperatures and practically none at the higher. One experimental point that agrees with the other data is the resistivity of 99.9983 percent pure aluminum at liquid-neon temperature in a zero field. These measurements were instrumental in the choice of aluminum for the large neon-cooled electromagnet previously described.

SUMMARY

The low-temperature, high-field-strength facilities of the Lewis Research Center, consisting of two copper water-cooled solenoids in the 100-k gauss range, are being used to investigate fundamental properties of materials at low temperatures and in high magnetic fields. A large cryogenically cooled, aluminum solenoid is being built and installed that will substantially increase the volume and field strength available for this research. These experiments are concerned with superconductors and semiconductors of various kinds. Some of the data that have been obtained are presented. The research, with special emphasis on the critical constants of hard superconductors, is being continued.

REFERENCES

1. Fakan, John C.: The Homopolar Generator as an Electromagnet Power Supply. High Magnetic Fields. Proc. Int. Conf. on High Magnetic Fields, M.I.T., Nov. 1-4, 1961, p. 210.

2. Laurence, J. C., and Brown, G. V.: A Large Liquid - Neon-Cooled Electromagnet. High Magnetic Fields. Proc. Int. Conf. on High Magnetic Fields, M.I.T., Nov. 1-4, 1961, p. 170.

3. Callaghan, Edmund E.: Taming the Supermagnets. Machine Design, Feb. 14, 1963.

4. Powell, John R., and Jacobs, Robert B.: Transverse Magnetoresistance of High Purity Aluminum from 4° K to 30° K. Unpublished NBS report.

TABLE I. - SPECIFICATIONS OF WATER-COOLED MAGNETS

Specification	5-cm bore	10-cm bore
Number of turns	24	20
Thickness of turns, cm	0.95	2.032
Spacing between turns, cm	0.064	0.102
Packing fraction	0.94	0.97
Dimensions, cm	5 I.D., 40 O.D.	10 I.D., 50 O.D.
α	8.00	5.0
β	4.85	4.2
Space inside liquid helium dewar, cm	1.6	6.0
Space inside magnet core at room temperature, cm	4.6	8.9
Maximum field, k gauss	110	88.5
Current, k amp	90	150
Voltages (total), v	18	13.8
Voltage between turns, v	0.6	0.7
Cooling-water flow rate (at 60 psi), lb/sec	10.2	40
Cooling-water temperature rise, ^{o}C	22	13
Field-current ratio, gauss/amp	1.15	0.59
Energy stored/volume, j/cm^3	47.9	31.00

TABLE II. - SPECIFICATIONS OF CRYOGENICALLY COOLED ALUMINUM MAGNET

Specification	Design	Accomplished at present
Number of coils	12	2
Number of turns/coil	75	72
Packing fraction	0.5	0.46
Dimensions, cm	30 I.D., 90 O.D	30 I.D., 90 O.D
α	3.0	3.0
β	4.8	0.8
Space inside liquid helium dewar, cm	25.7	25.7
Space inside magnet core at room temperature, cm	25.7	25.7
Maximum field, k gauss	200	48.6
Maximum current, k amp	15.2	10.8
Voltage (total), v	30.6	3.84
Power consumed, kw	460	41.4
Room-temperature resistance, ohms	0.200	0.070
Liquid-hydrogen resistance, ohms	0.002	[a] 2.5×10^{-4}
Field-current ratio, gauss/amp	--	4.5
Energy stored/volume, j/cm^3	--	9.4

[a] Includes a factor of approximately 2 for magnetoresistance.

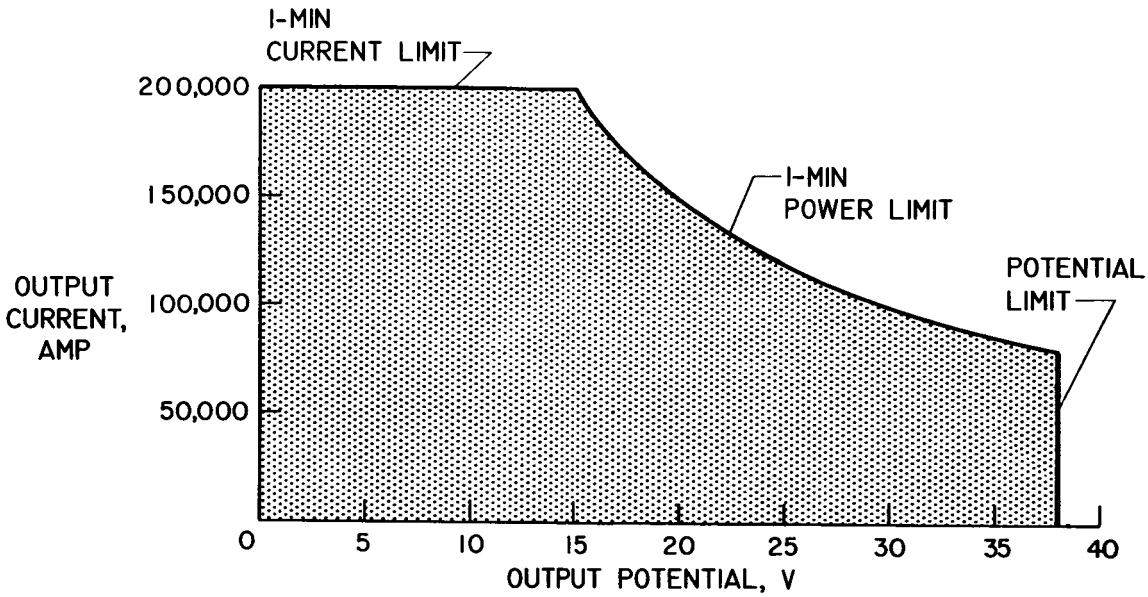

Fig. 1. - Characteristics of homopolar machine.

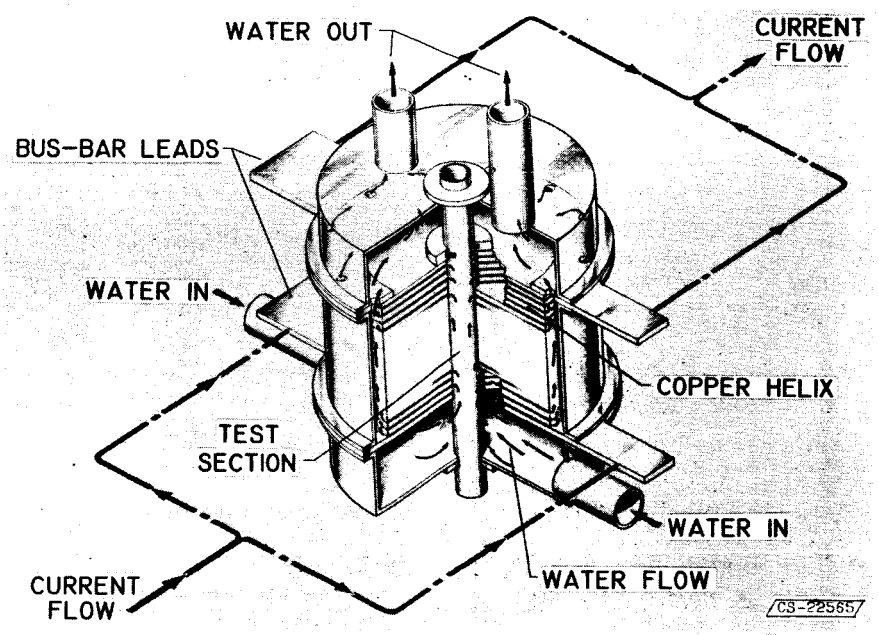

Fig. 2. - Construction of water-cooled magnets.

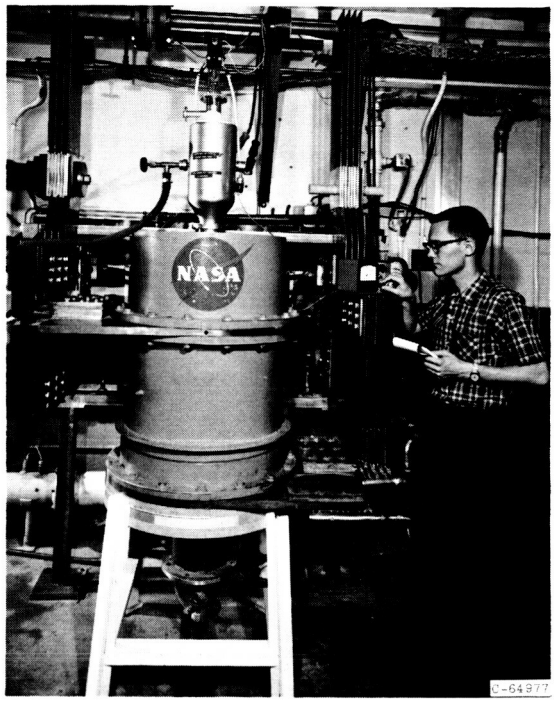

Fig. 3. - Photograph of 10-cm water-cooled electromagnet.

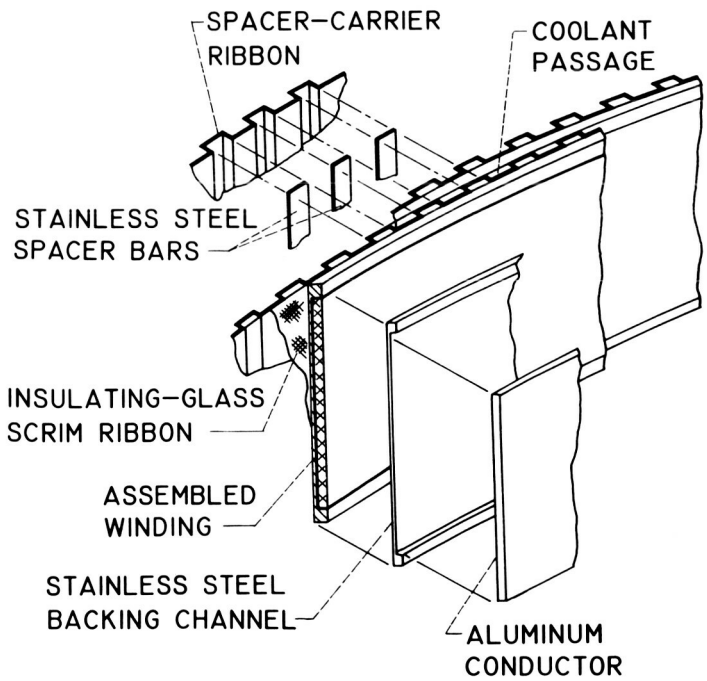

Fig. 4. - Construction of coils of cryogenically cooled aluminum magnet.

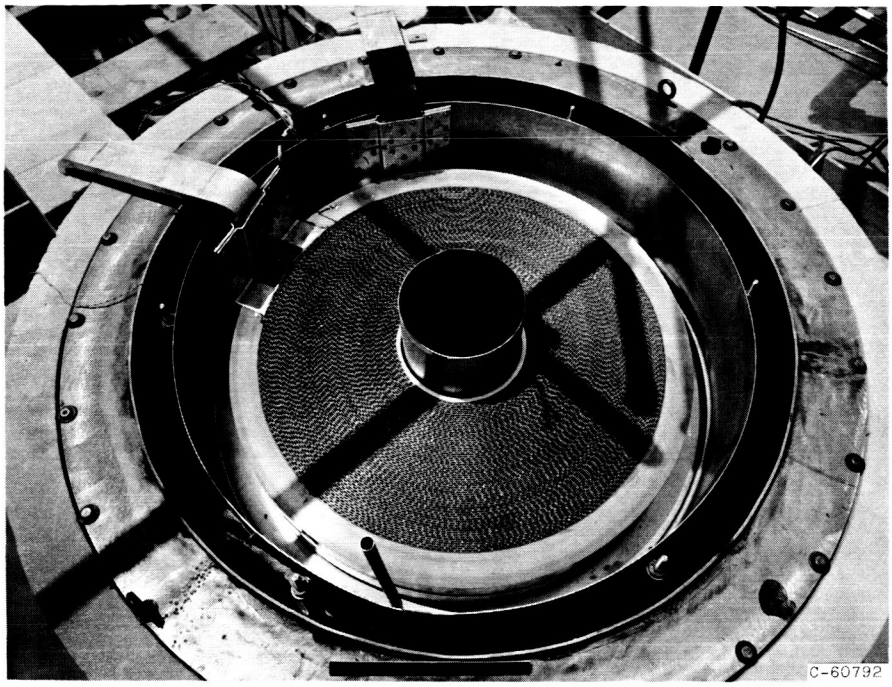

Fig. 5. - Coils in dewar.

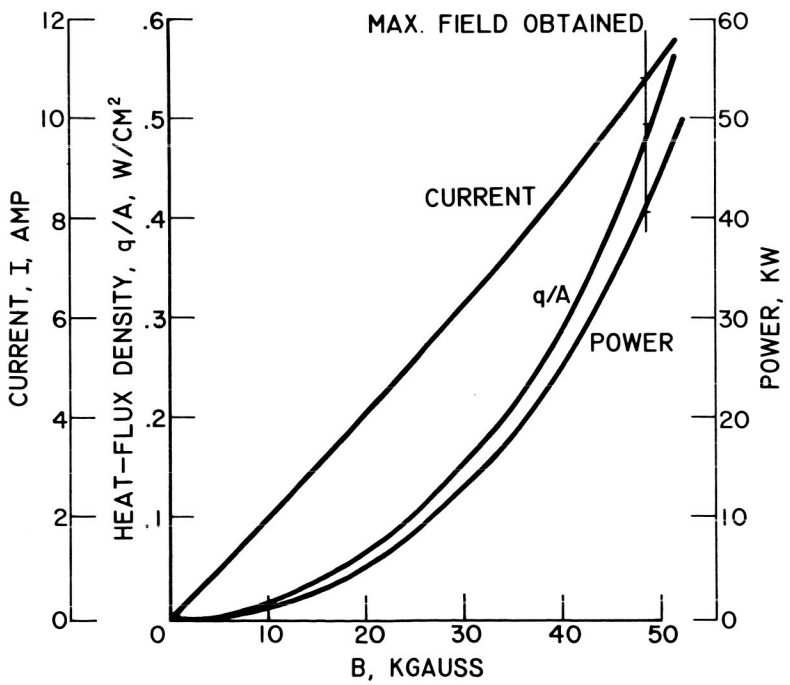

Fig. 6. - Performance characteristics of aluminum magnet. Magnetic field, two coils; coolant, liquid hydrogen.

Fig. 7. - Bottom view of neon-cooled electromagnet containment vessel.

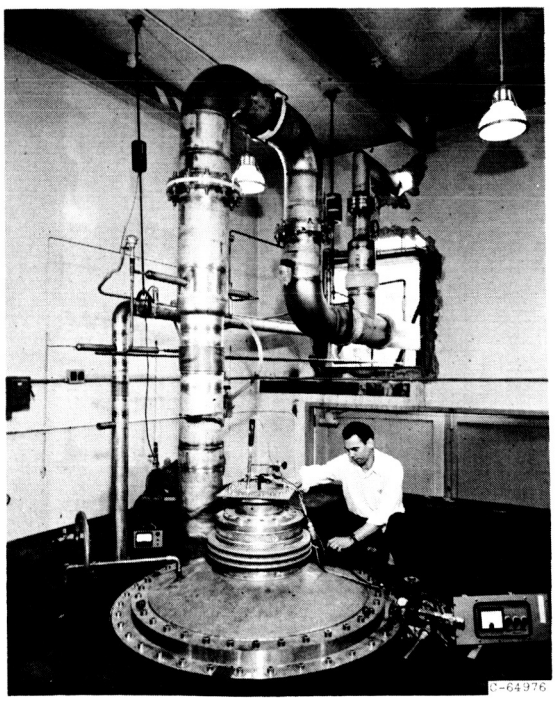

Fig. 8. - Top view of neon-cooled electromagnet containment vessel.

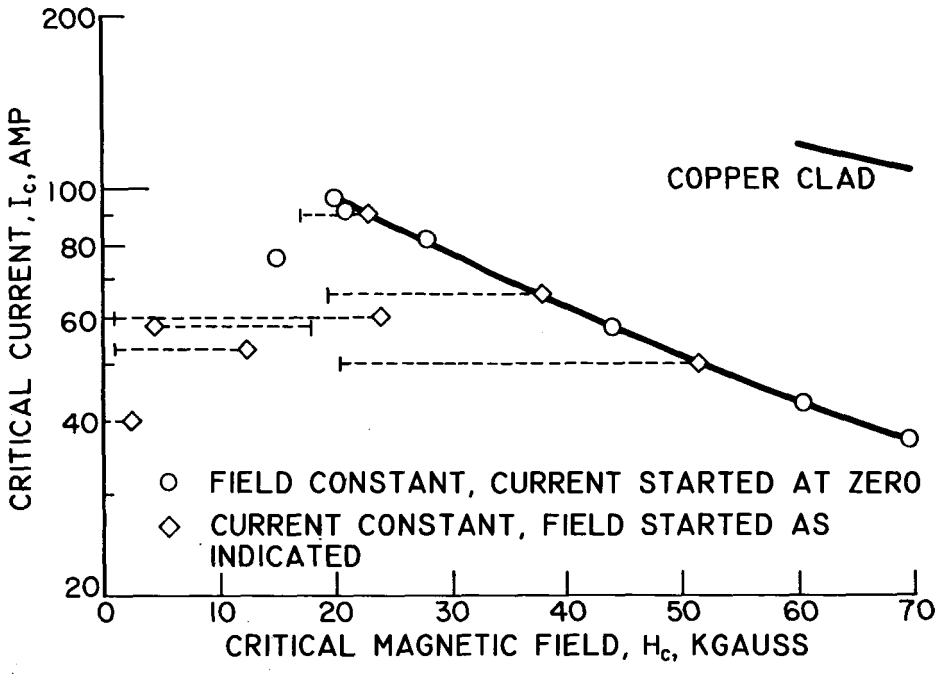

(a) Sample HDC-A.

Fig. 9. - Critical current as function of critical field for Nb_3Sn ribbon.

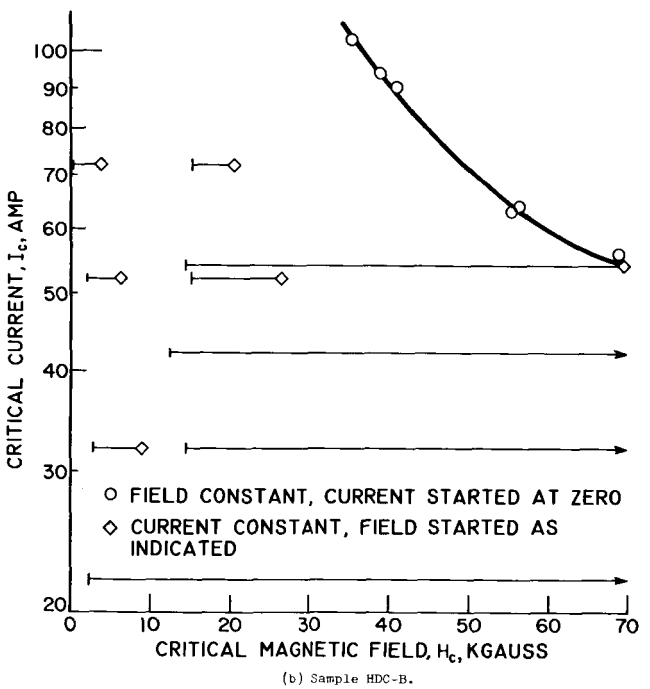

(b) Sample HDC-B.

Fig. 9. - Concluded. Critical current as function of critical field for Nb_3Sn ribbon.

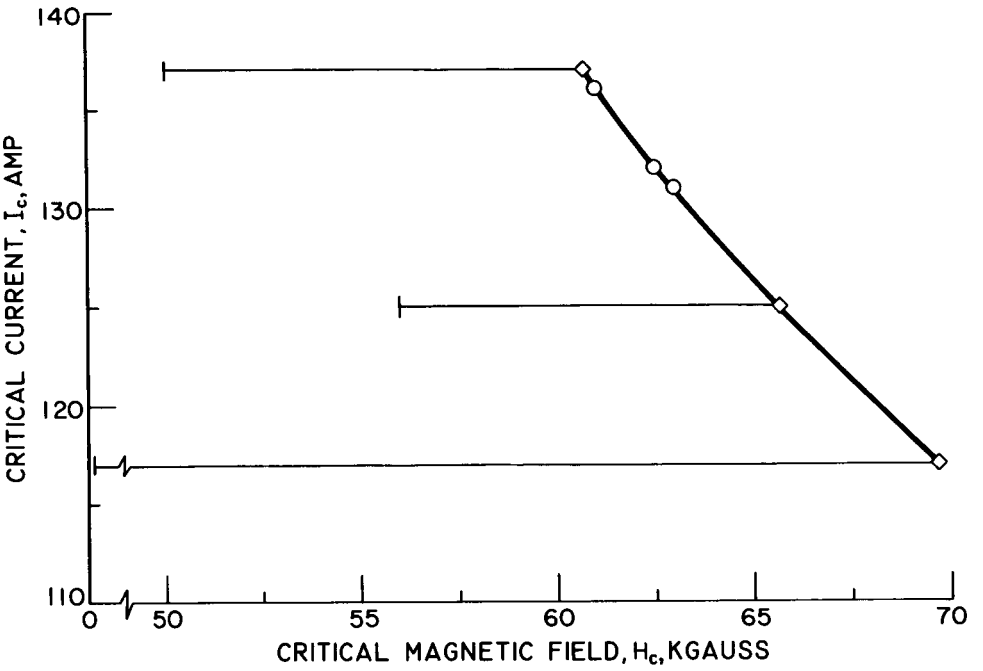

Fig. 10. - Critical current as function of critical field for copper plated Nb_3Sn ribbon.

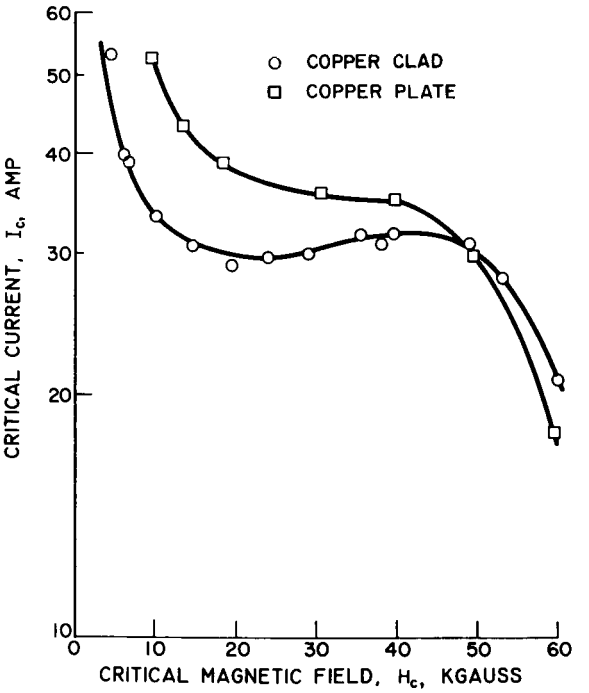

Fig. 11. - Critical current as function of critical field for Nb(25)Zr wire.

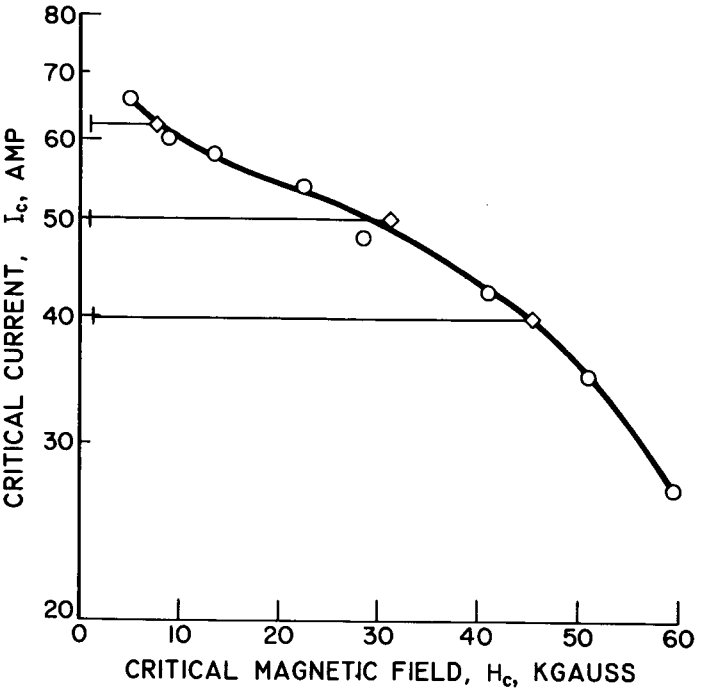

Fig. 12. - Critical current as function of critical field, copper plated Nb(33)Zr wire.

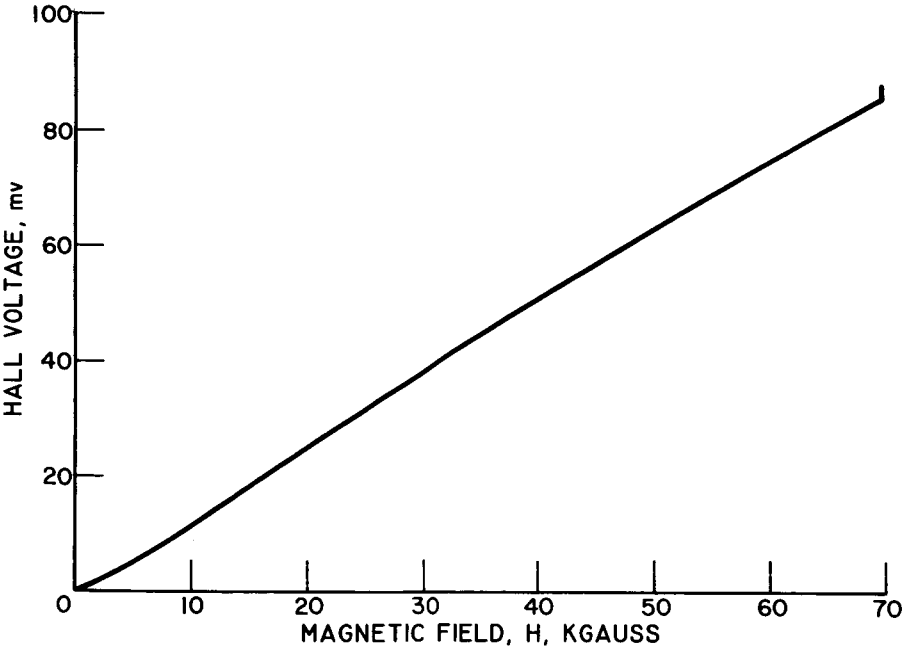

(a) Room temperature.

Fig. 13. - Response of Hall-effect device as a function of externally applied magnetic field.

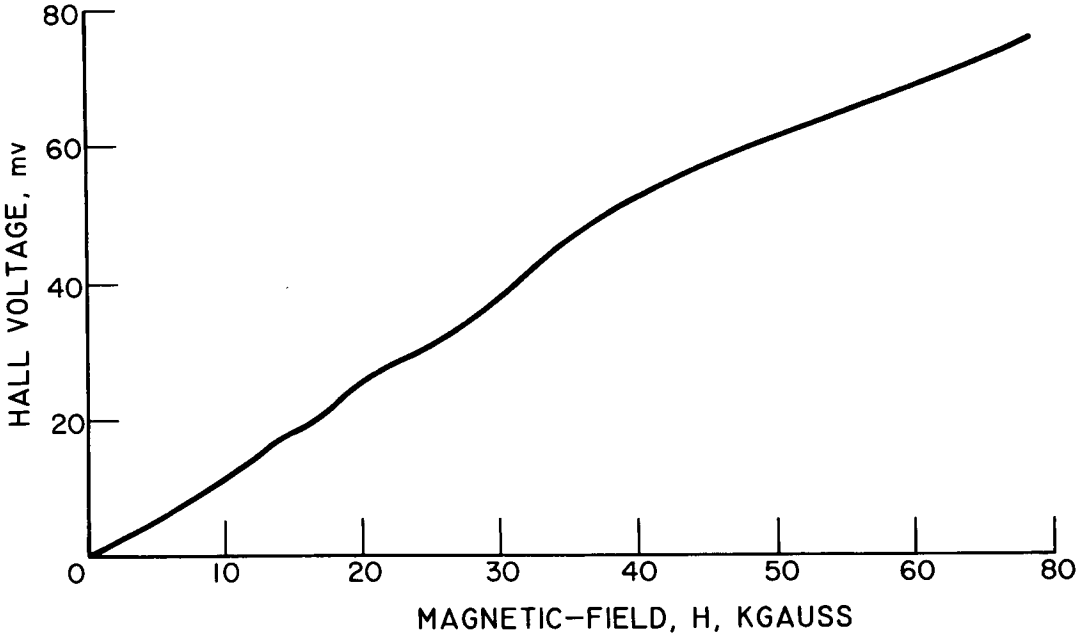

(b) Liquid-helium temperature.

Fig. 13. - Concluded. Response of Hall-effect device as a function of externally applied magnetic field.

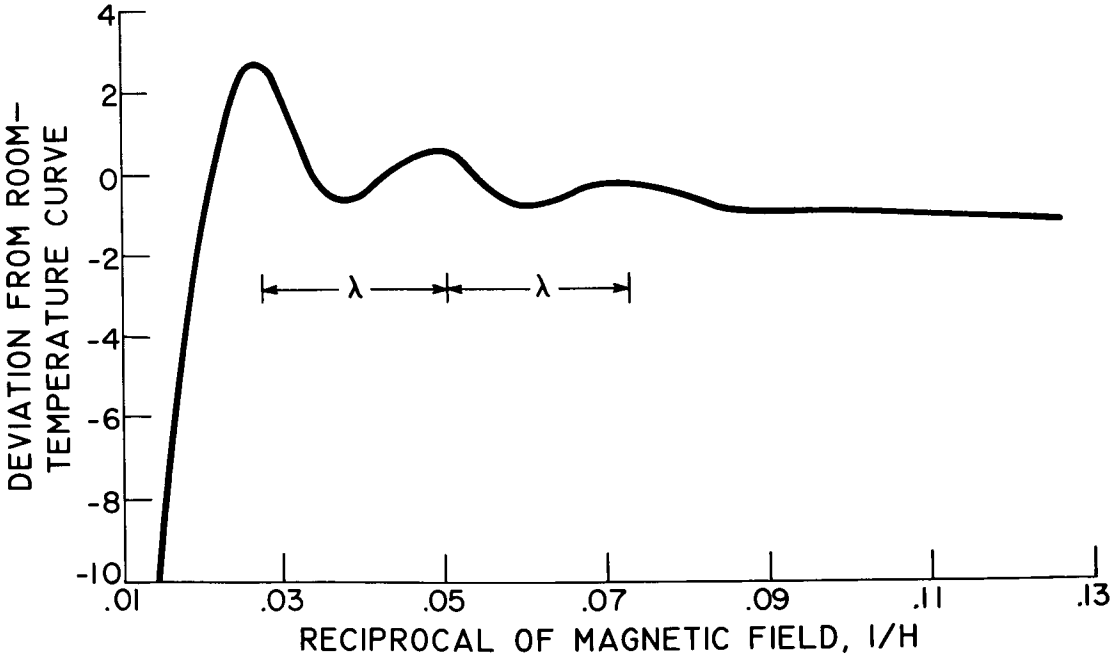

Fig. 14. - Deviation of voltage output of Hall-effect device at 4.2° K from linear output at room temperature.

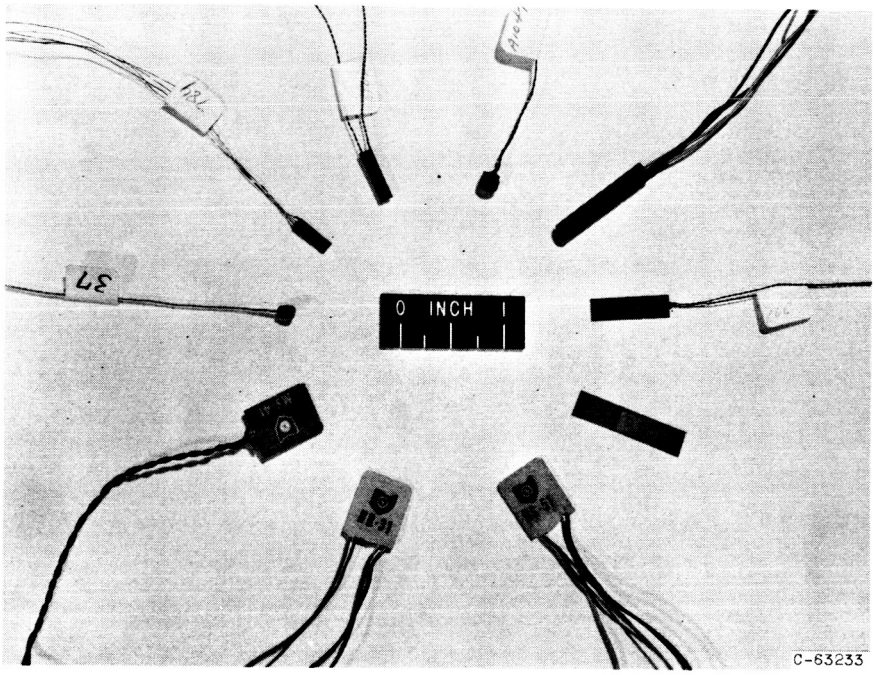

Fig. 15. - Commercial Hall-effect device.

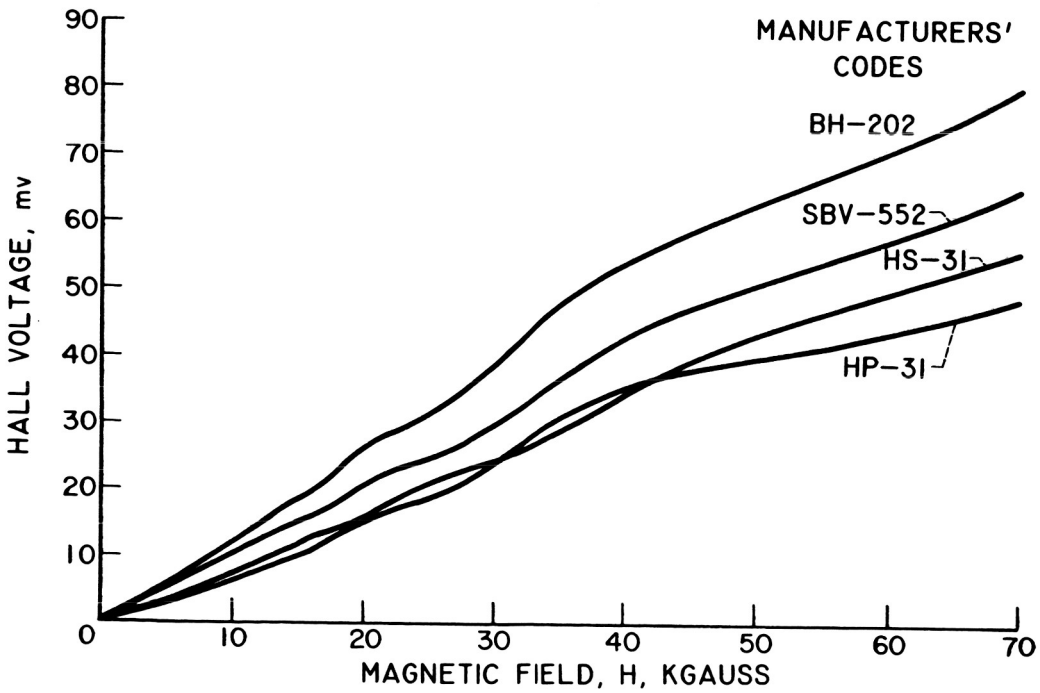

Fig. 16. - Response of Hall-effect devices at 4.2° K as a function of externally applied magnetic field.

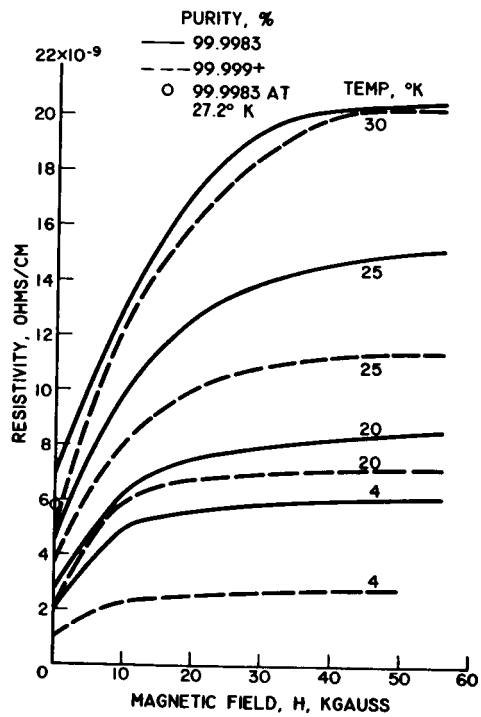

Fig. 17. - Magnetoresistance of aluminum.